In vivo tissue compatibility of two radio-opaque polymeric biomaterials

ELSEVIER

PII S0142-9612(96)00085-3

Biomaterials **18** (1997) 31–36

0142-9612/97/$17.00

In vivo tissue compatibility of two radio-opaque polymeric biomaterials

Marc-Anton B. Kruft*†, Frederik H. van der Veen‡ and Leo H. Koole*

*Centre for Biomaterials Research, University of Maastricht, P.O. Box 616, 6200 MD Maastricht, The Netherlands;
†Eindhoven Polymer Laboratories (EPL), Eindhoven University of Technology, Eindhoven, The Netherlands;
‡Department of Cardiology, University of Maastricht, Maastricht, The Netherlands

Polymeric biomaterials featuring intrinsic radio-opacity continue to attract considerable scientific attention. This work focusses on two polymers that contain covalently bound iodine, rendering the materials radio-opaque. The first material is hard, transparent and glass-like, and consists of methyl methacrylate, 2-(2′-iodobenzoyl)-ethyl methacrylate (**1**) and 2-hydroxyethyl methacrylate (HEMA), in the molar ratio 65 : 20 : 15, respectively. The second material is a cross-linked hydrophilic network, consisting of HEMA and **1**, in the molar ratio 80 : 20, respectively. Both materials were characterized by means of different physico-chemical techniques, including magic-angle-spinning solid state NMR spectroscopy, infrared spectroscopy and differential scanning calorimetry. Moreover, both materials were implanted subcutaneously in rats for 24 days. Upon explantation and histological examination, it appeared that both materials are well tolerated. No tissue necrosis, abscess formation or inflammation were observed. The samples were found to be surrounded by a vascularized capsule consisting of connective tissue cells. The results reveal excellent tissue compatibility for both materials. This is an important observation, since tissue compatibility is absolutely necessary for the applications which are foreseen for this type of radio-opaque biomaterials. © 1996 Elsevier Science Limited

Keywords: Radio-opacity, biocompatibility, tissue compatibility, radio-opaque biomaterials

Received 12 February 1996; accepted 6 May 1996

When a polymeric biomaterial is to be placed inside the human body, it is often made radio-opaque through addition of an X-ray absorbing additive, such as barium sulphate or zirconium dioxide[1,2]. Examples are found amongst biomaterials for temporary use (e.g. polyurethane catheters for epidural anaesthesia) and also amongst long-term implants (e.g. methacrylic bone cement or denture base). The most important drawback associated with the use of radio-opaque additives is that the physico-mechanical properties of the polymeric matrix are compromised. This is hardly a surprise if one realizes that:

1. Radio-opaque fillers are mixed to appreciably high concentrations (methacrylic bone cements like Palacos® or Simplex® P contain approximately 7% barium sulphate by weight).
2. Thermodynamics dictate that inorganic salts do not mix with organic materials.

For methacrylic bone cements, it has been reported that the barium sulphate particles tend to form clumps, which influence the rate of formation and/or propagation of mechanical defects[3]. For polyurethane catheters, it is known that addition of barium sulphate has a substantially negative influence on the smoothness and lubricity of the inner and outer surfaces. Usually, 40–60% barium sulphate (by weight) is required to impart sufficient contrast in catheters, since the wall thickness is only of the order of several tenths of a millimetre.

In recent years, several groups, including ourselves, have worked on a new type of radio-opaque polymeric biomaterial, following an approach which should circumvent problems associated with the use of a radio-opaque filler[4–11]. We reasoned that use of monomeric building blocks, which contain covalently bound iodine, will afford polymers which exhibit intrinsic radio-opacity. Several methacrylate-type iodine-containing monomers were prepared in our laboratory, and structures **1–4** are representative examples.

Co/terpolymerizations of these building blocks with other methacrylates, such as methyl methacrylate (MMA) and 2-hydroxyethyl methacrylate (HEMA), were found to proceed smoothly. Co/terpolymers with high molecular weight ($M_w > 100\,kg\,mol^{-1}$) and satisfactory polydispersion (M_w/M_n in the range 2–3) can be made in laboratory-scale bulk polymerization reactions. Compound **1** was found to be very suitable for this purpose, since it is readily accessible. Furthermore, we have recently found that the reactions **1** + MMA and **1** + HEMA afford random-type copolymers[12].

Correspondence to Dr L.H. Koole.

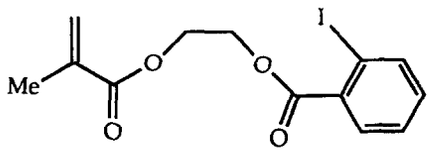

1

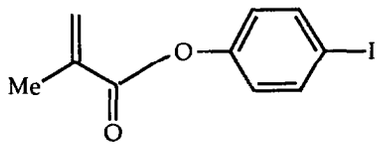

2

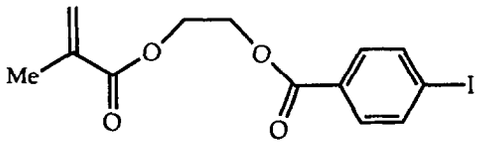

3

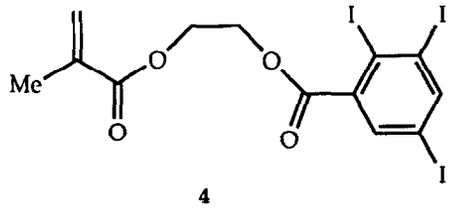

4

Several future applications for polymeric biomaterials derived from building blocks like **1–4** can be expected, for instance:

1. For the construction of a new type of all-polymeric endovascular stent, which uniquely combines radio-opacity with enhanced biocompatibility (especially blood compatibility) as compared to metals.
2. As a constituent of a new type of methacrylic bone cement with the unique feature that the contrasting component contributes to the cement's integrity.
3. As a constituent of an intracorporeal drug reservoir from which the drug diffuses slowly into body fluids, and which can be recharged since the reservoir can be precisely located through X-ray fluoroscopy.

As a part of our ongoing research on iodine-containing biomaterials, we now report on their *in vivo* tissue compatibility. Two representative materials were chosen. The first is the terpolymer consisting of MMA, HEMA and **1**, in the molar ratio 65 : 15 : 20, respectively. This material is designated as an attractive candidate for the construction of an all-polymeric endovascular stent, because of its low surface thrombogenicity *in vitro*, its excellent radio-opacity, and because of the possibility of processing this material into complex shapes, e.g. through injection moulding[10]. The second material is a new radio-opaque cross-linked hydrogel, consisting of HEMA and **1** in the molar ratio 80 : 20. This material was chosen in view of its possible utility for slow drug release purposes *in vivo*; tissue compatibility is an essential requirement with regard to this application.

MATERIALS AND METHODS

The terpolymer MMA–HEMA–**1** (molar ratio 65 : 15 : 20, respectively) was prepared as described previously[10]. The material was compression moulded at 180°C using a Fontijne press (Fontijne, Vlaardingen, The Netherlands). This afforded rectangular plates, with a thickness of approximately 2 mm. Out of these plates, two types of small squares were machined. Their dimensions were: small, $5.5 \times 5.5 \times 1.7\,mm^3$; large, $7.5 \times 7.5 \times 1.7\,mm^3$. The surfaces of the squares were carefully polished, avoiding the use of any oils or lubricants. The squares were then gas-sterilized (ethylene oxide) at about 55°C and stored in dry form.

Synthesis of the cross-linked network started out with careful purification of the starting materials. HEMA was distilled *in vacuo* as described earlier[8,10]. Monomer **1** was prepared through reaction of 2-iodobenzoyl chloride and HEMA, and purified via chromatography on a silica gel column[10]. *N,N*-Dimethyl formamide (DMF) was distilled from lithium aluminium hydride, and stored over 4 Å molecular sieves. Tetraethyleneglycol dimethacrylate (purity > 99.0%) and 2,2′-azobisisobutyronitrile (AIBN; purity > 99.5%) were purchased from Aldrich and used without further purification.

HEMA (2.95 g, 22.7 mmol), **1** (2.05 g, 5.7 mmol), tetraethyleneglycol dimethacrylate (75.7 μmol), AIBN (158.7 μmol) and 10 ml of DMF were combined in a 50-ml round-bottomed flask. Magnetic stirring resulted in a clear homogeneous solution. Highly pure argon gas was led through a glass capillary and gently bubbled through the monomer solution for 5 min. This solution was transferred into a cylindrical Teflon mould (diameter = 20 mm, height = 5 mm). The mould was sealed and placed in a thermostatted oil bath, equipped with a programmable time–temperature control system (PM Lauda, Koningshofen, Germany). The program consisted of four steps of 10 h at 40, 50, 60 and 70°C, consecutively. After completion of this procedure, the transparent gel was removed from the mould and immersed in a beaker containing deionized water. Within 30 min, the gel showed a colour change from transparent to opaque (white). The contents of the beaker were stirred for 1 week, with two water exchanges daily. Then, the gel was cut into pieces ($4 \times 4 \times 1\,mm^3$), which were immersed in pure ethanol for 1 h. The gel pieces were washed with sterile phosphate-buffered saline (PBS). Subsequently, the gel pieces were stored at 37°C in sterile PBS. Elemental analysis of the wet polymeric network being washed with deionized water showed the

absence of any trace of nitrogen, which corresponds to the absence of the solvent, DMF.

Elemental analysis

Elemental analysis was performed by Galbraith Laboratories (Knoxville, TN, USA).

Solid-state NMR

Solid-state ^{13}C-NMR measurements were carried out on a Bruker MSL 400 Fourier Transform NMR spectrometer (Bruker Analytische Messtechnik, Rheinstetten, Germany) at 100.6 MHz. Samples of *ca* 250 mg were measured in 4 mm o.d. rotors made of ZrO_2 of the Bruker double-bearing type. The proton 90° pulse length was 6.6 μs and the repetition time 1 s. Magic-angle-spinning rates were 5.5 and 7.0 kHz; 4800 free induction decays with an acquisition time of 20 ms were accumulated in 1 k data points. During acquisition ^{1}H decoupling was carried out.

Fourier transform infrared spectroscopy

Infrared spectra were recorded with a Mattson Polaris spectrometer equipped with a standard DTGS detector and He/Ne laser. The spectra were obtained after accumulation of 25 scans between 4000 and 400 cm^{-1}. The sample compartment was held at room temperature and under a nitrogen atmosphere.

Differential scanning calorimetry

The glass-transition temperature (T_g) was measured using a heating rate of 10°C min^{-1} using a Perkin–Elmer DSC 7 (Perkin–Elmer Inc., USA). T_g values of the polymeric network in both the dry and wet states (PBS) were determined from the first heating scan. T_g was taken as the midpoint of the transition region. Argon was used as the carrier gas. The differential scanning calorimeter was calibrated using indium and zinc.

Transmission electron microscopy

Small pieces of the hydrogel (equilibrated with water) were prepared for transmission electron microscopy (TEM; Philips CM 12, Eindhoven, The Netherlands). The pieces were frozen in liquid ethane and cut into ultra-thin sections (150 nm) using a cryomicrotome (Cryonova LKB, LKB-Produkter, Sweden) at −120°C. Subsequently, the sections were mounted on copper grids and transferred into the microscope with a Gatan

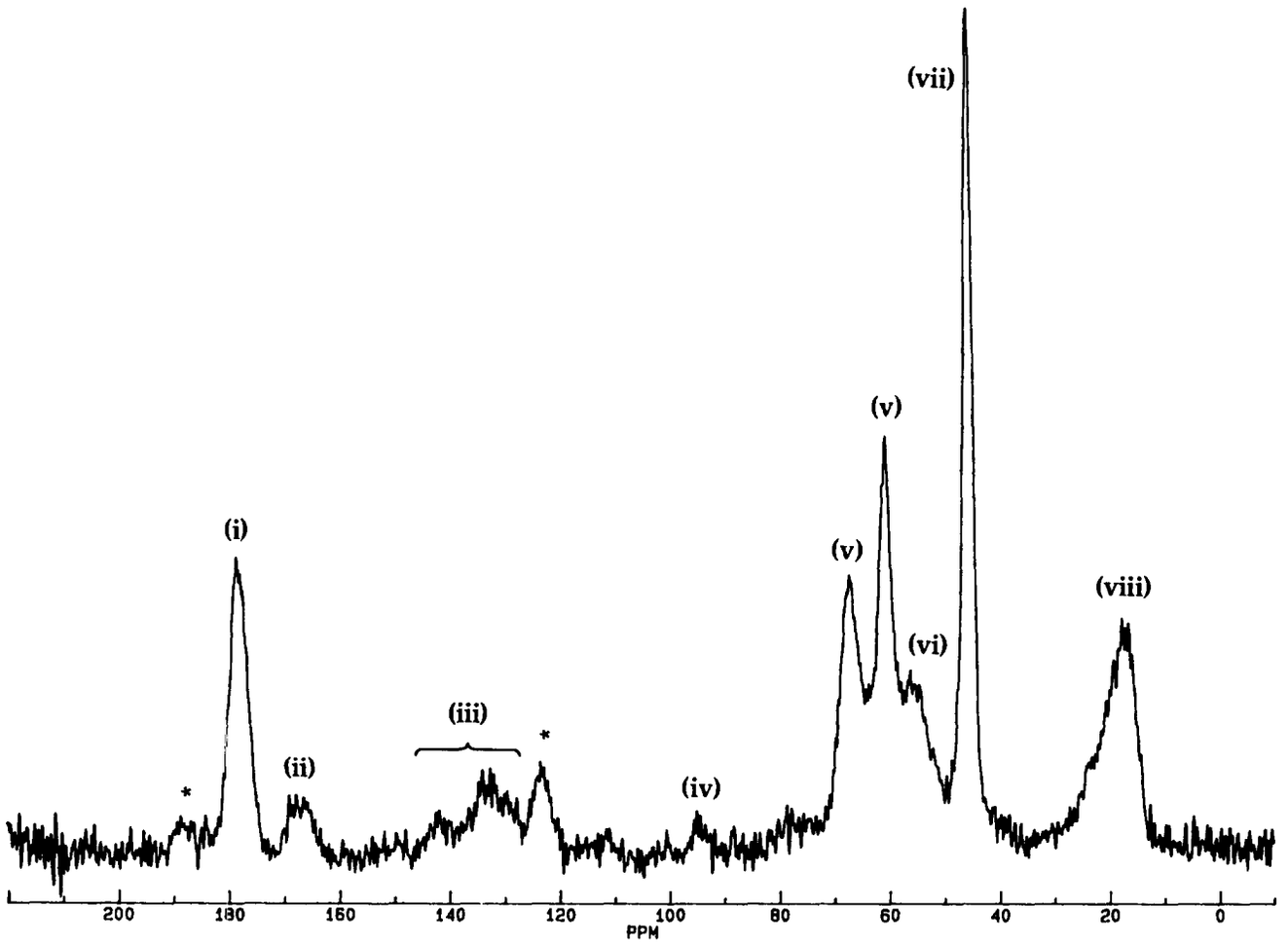

Figure 1 Solid-state ^{13}C-NMR spectrum of radio-opaque polymeric network in the dry state (cross-polarization, magic-angle, 5.5 kHz). The most important spinning side-bands are indicated with asterisks. Signals and spinning side-bands were distinguished unequivocally via a comparison with the analogous spectrum, recorded at a spinning frequency of 7 kHz. Assignments are as follows: (i) C=O groups, attached to the polymer chains; (ii) C=O groups of 2-iodobenzoyl; (iii) aromatic carbons, except C–I; (iv) aromatic carbon, attached to iodine; (v) OCH_2 of HEMA building blocks and OCH_2 of **1** building blocks; (vi) CH_2 groups of the polymeric chains; (vii) quaternary carbons in the polymer chains; (viii) methyl groups, attached to the polymer chains.

Cryo-holder. After observation of the sections at a temperature of −170°C, the sections were freeze-dried at a temperature of −80°C (pressure = 8×10^{-5} Pa) and observed again.

Evaluation of tissue compatibility

Five female Lewis rats aged 6 weeks (weight 110–120 g) were used. In each rat, 100 mg ampicillin (antibiotic) was injected subcutaneously, then the rats were anaesthetized using nembutal (0.1 ml per 100 g body weight). Subsequently, a small incision on the skin was performed for introduction of the polymer. In each animal, three radio-opaque polymer specimens were implanted: one small square (terpolymer), one large square (terpolymer) and a square consisting of the hydrogel. The piece of hydrogel was implanted proximally, large square centrally and small square distally, all on the back of the rat. Subcutus was closed by vicryl 4-0, whereas the skin was secured with Mersilene 2-0 suture. The rats were caged and had free access to standard rat food and water. The Dutch national guidelines for animal welfare were observed. Before killing, the rats were anaesthetized using nembutal (0.1 ml per 100 g body weight). The implants were extirpated from the animals at 24 days. After killing the animals, the implants with their surrounding tissues were excised immediately, fixed in 4% buffered formalin and embedded in paraffin. Sections of paraffin-embedded specimens, with an average thickness of 6 μm, were stained with haematoxylin–eosin and investigated using light microscopy (Zeiss, Axio Shop, Germany).

RESULTS

Physico-chemical characterization of the radio-opaque network

Figure 1 shows the solid-state ^{13}C-NMR spectrum of the radio-opaque polymeric network in the dry state at a magic-angle-spinning rate of 5.5 kHz. The spectrum consists of eight signals and clearly reveals the identity of the polymeric network. Note especially signal iv, which originates from the aromatic carbon covalently bound to iodine. This characteristic signal is relatively low, since only 20 mol% of building block **1** was incorporated into the polymeric network. Since only a small amount of cross-linker was used, no characteristic signals of the cross-linker can be observed in the spectrum. In fact, the solid-state ^{13}C-NMR spectrum of the network is comparable with the spectrum of the radio-opaque terpolymer, as described in Ref. 10. This is due to the similarity in building blocks of both terpolymer and hydrogel.

Fourier transform infrared (FT-IR) spectra of the polymeric network in the dry state showed the following characteristic signals, and also confirmed the identity of the network: 3589–3232, broad (OH); 1732 (C=O); 1589 and 1446 (C=C, aromatic); 1018 (primary alcohol) cm^{-1}.

T_g values found for the polymeric network are 68°C in the dry state and 33°C after equilibrium in PBS. The lowering of the T_g is the result of the plasticizing effect of water. Since a T_g value of 33°C is found for the network in PBS, it will be in a rubbery state in physiological conditions (PBS, 37°C).

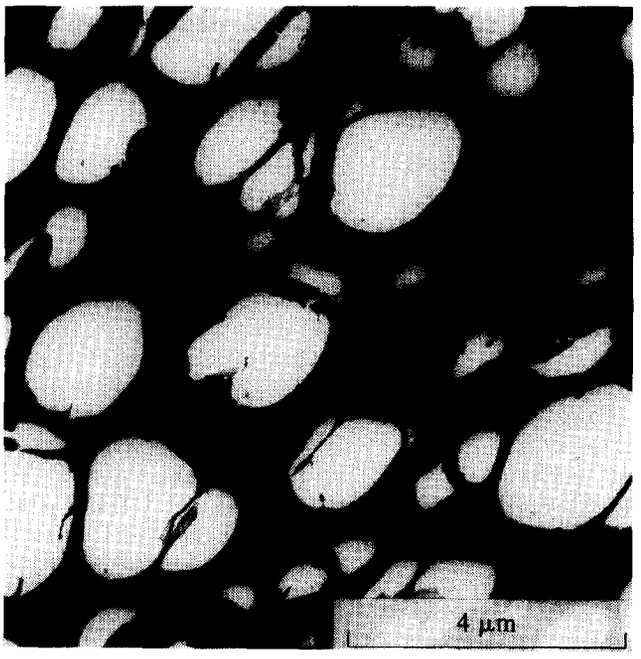

Figure 2 Representative transmission electron micrograph of a piece of hydrogel subjected to freeze-drying.

The equilibrium water content of the gel was determined at a temperature of 37°C by drying and reweighing. The equilibrium water content (H in %) was calculated using the following equation:

$$H = 100 \times (W_1 - W_2)/W_1$$

where W_1 and W_2 represent the weight of the fully hydrated gel and the dry gel, respectively. Three square-like specimens of the hydrogel were taken, and equilibrium was reached when three consecutive measurements gave the same weight. An equilibrium water content of 55.0 ± 2.7% was found. Comparing this value of the equilibrium water content with the value as reported for pHEMA (H = 62.4%, T = 30°C)[4], it may be concluded that, despite the partial introduction (20 mol%) of building block **1** in the polymeric network, its swelling ability is not significantly affected. This is important to note since it has been reported that in the case of the iodinated pHEMA microspheres, the swelling was impeded significantly[13].

Porosity of the radio-opaque hydrogel was determined by TEM. An average pore diameter of 1.9 μm was found. *Figure 2* shows a representative transmission electron micrograph of a piece of hydrogel subjected to freeze-drying. Furthermore, TEM showed that the pores in the gel are not interconnected. No significant differences could be found when comparing the pore diameters of coupes subjected and not subjected to freeze-drying.

Tissue compatibility of the terpolymer and hydrogel

Microscopic evaluation of the explants showed that all samples were well tolerated by the subcutaneous tissues. In tissue surrounding the implanted materials, tissue necrosis, abscess formation or acute inflammation were not observed. Furthermore, no tissue reactivity or cellular mobilization occurred in areas

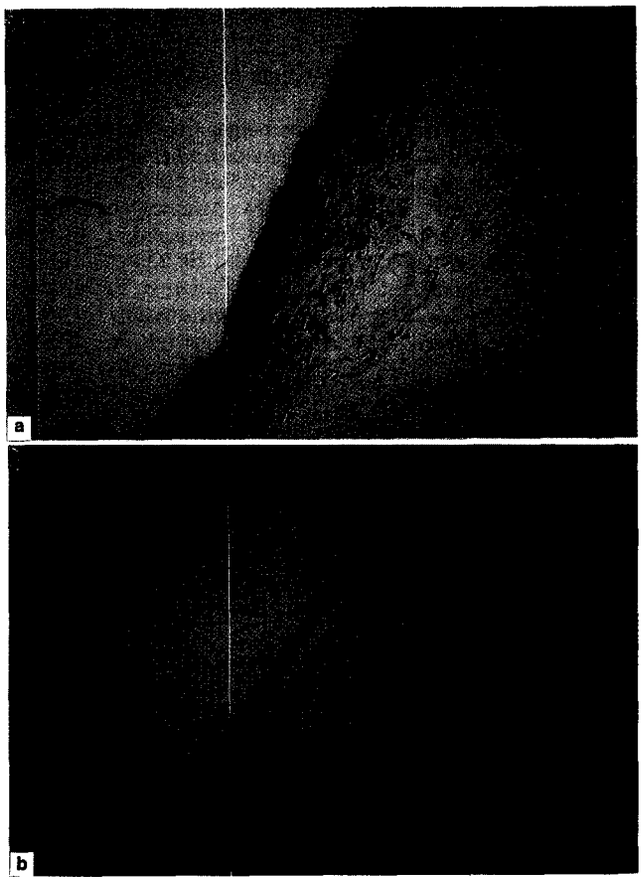

Figure 3 Representative photographs of histological sections of the interface between the two different polymeric materials and surrounding tissue. **a**, Interface of small square of terpolymer. Original magnification ×20. **b**, Interface of piece of hydrogel. Original magnification ×10.

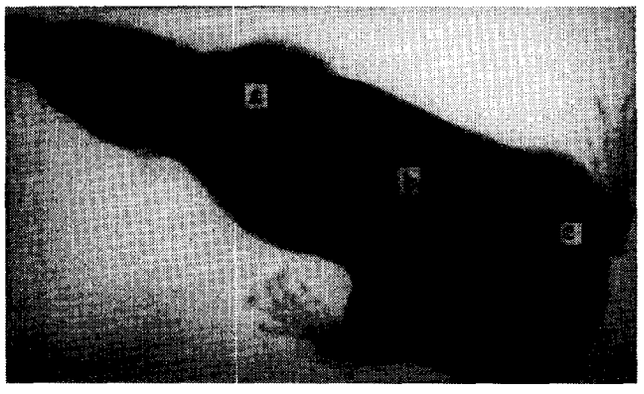

Figure 4 Representative X-ray image of a rat bearing the three different test specimens: the piece of hydrogel, **a**, was implanted proximally, a large square, **b**, centrally and a small square, **c**, distally, all on the back of the rat. The position of the specimens is clearly X-ray visible.

remote from the implantation site. The samples were surrounded by a vascularized connective tissue capsule, with a variable thickness of two to 10 cell layers. The capsule consisted of connective tissue cells, including small vessels, fibroblasts and lymphocytes.

Representative photographs of histological sections of the interface between the two different polymeric materials and surrounding tissue are shown in *Figure 3*; one image shows the interface of a small square (terpolymer; *Figure 3a*), the other shows the interface of a piece of hydrogel (*Figure 3b*). No differences in tissue response between terpolymer and hydrogel were observed.

The rats ($n = 5$) with implanted specimens were submitted to fluoroscopy (clinical conditions) after 9 days of implantation. X-ray images of all rats clearly showed the position of the specimens. One representative X-ray image of a rat bearing the test specimens is shown in *Figure 4*.

As can be seen in *Figure 4*, the shape and location of both hydrogel and terpolymer (i.e. small and large squares) are clearly discernible under the X-ray camera. Moreover, *Figure 4* shows that the squares are better X-ray visible than the gel. This is due to more iodine per unit volume for the terpolymer as compared to the hydrogel. Note that both hydrogel and terpolymer consist of 20 mol% of building block **1**.

DISCUSSION

The mechanisms behind acceptance and/or integration of implant biomaterials are complex and still poorly understood. This point deserves attention, since no implanted artificial material can be considered totally inert. According to Hench and Wilson[14], four major categories of host responses can be distinguished:

1. The material releases some toxic compounds, leading to necrosis of surrounding tissue.
2. The material is non-toxic, but is gradually being resorbed and replaced by the surrounding tissue.
3. The material is non-toxic and biologically inactive, but cannot be degraded by the host, which reacts by encapsulation.
4. The material is non-toxic, but highly interactive with the surrounding tissues in forming (chemical) bonds with it. These interactions stabilize the implant.

Obviously, our observations with the squares of both radio-opaque plastics (hard terpolymer and the hydrogel) fit into the third category. In all cases, encapsulation was indeed observed. No necrosis, abscess formation or acute inflammation were observed near the implants. In remote areas, no signs of tissue reactivity or cellular immobilization could be detected.

In our opinion, these results are of interest with respect to the evaluation of the possible utility of the radio-opaque polymers as implant biomaterials. However, considering the suggested application of the terpolymer as a construction material for endovascular stents, it is clear that the present results hardly have any predictive value. A stent is pressed against the (damaged) vascular wall after deployment, and should exert an inhibiting effect on proliferation of sub-endothelial cells. This proliferation is considered the most important risk factor with respect to restenosis, i.e. reocclusion of the vessel over a period of approximately 3–6 months after percutaneous transluminal (coronary) angioplasty and stent placement. It remains uncertain whether the radio-opaque terpolymer would behave better in this respect, if compared to the metallic stent materials currently

used. Further work, using a radio-opaque polymeric stent prototype in an *in vivo* damaged vessel wall model, is necessary to specifically address this point.

The data obtained with the radio-opaque hydrogel might have a greater predictive value. It can be expected that a material like the radio-opaque network can be used to construct a hollow container, which can be filled with a concentrated solution of a drug (e.g. gentamicin or 5-fluorouracil). After subcutaneous implantation, the drug can diffuse across the wall of the container, and be released into the subcutaneous tissue and body fluids. Since the material is radio-opaque and the container can be precisely located under X-ray fluoroscopy, it is conceivable that the container can be refilled *in situ* using a thin-needle syringe. Currently, we are working on the fabrication of such a polymeric, radio-opaque, porous and hollow sphere. Further work along this line, addressing issues like control of drug release from the container, acceptance and/or integration of the container *in vivo*, long-term biological stability of the material, optimizing the technique for recharging of the container, etc., is in progress in our laboratories.

CONCLUSIONS

Findings from this study show that the terpolymer and hydrogel combine two unique features, namely *in vivo* tissue compatibility and excellent *in vivo* radio-opacity. Especially in the field of biomaterials, the new radio-opaque materials offer many potential applications as construction material for catheters, guide-wires, bone cements, denture bases, drug release systems and cardiovascular devices.

ACKNOWLEDGEMENTS

We thank Mr L.J. van den Ven (Eindhoven University of Technology) for his help in obtaining the solid-state ^{13}C-NMR spectrum, Mr P. Kelderman (Central Animal Facilities, University of Maastricht) for his assistance with the animal experiments and Mr P. Bomans for the transmission electron microscopic observations (Electron Microscopy Unit, University of Maastricht).

REFERENCES

1 Williams DF, Roaf R. *Implants in Surgery*. London: WB Saunders, 1973: 132–134.
2 Mark HF, Bikales NM, Overberger CG, Menges G, eds. *Encyclopedia of Polymer Science and Engineering*, 2nd edn, Vol. 14. New York: John Wiley, 1988: 1–8.
3 Bhambri SK, Gilbertson LN. Micromechanisms of fatigue crack initiation and propagation in bone cement. *J Biomed Mater Res* 1995; **29:** 233–237.
4 Jayakrishnan A, Chithambara Thanoo B, Rathinam K, Moharty M. Preparation and evaluation of radio-opaque hydrogel microspheres based on pHEMA/iothalamic acid and pHEMA/iopanoic acid as particular emboli. *J Biomed Mater Res* 1990; **24:** 933–1004.
5 Jaykrishnan A, Chithambara Thanoo B. Synthesis and polymerization of some iodine-containing monomers for biomedical applications. *J Appl Polym Sci* 1992; **44:** 743–748.
6 Moszner N, Salz U, Klestner AM, Rheinberger V. Synthesis and polymerization of hydrophobic iodine-containing methacrylates. *Angew Makromol Chem* 1995; **224:** 115–123.
7 Davy KWM, Causton BE. Radio-opaque denture base: a new acrylic co-polymer. *J Dent* 1982; **10:** 254–264.
8 Kruft MAB, Benzina A, Bär F *et al.* Studies on two new radio-opaque polymeric biomaterials. *J Biomed Mater Res* 1994; **28:** 1259–1266.
9 Benzina A, Kruft MAB, Bär F *et al.* Study on a new radio-opaque polymeric biomaterial. *Biomaterials* 1994; **15:** 1122–1128.
10 Kruft MAB, Benzina A, Blezer R, Koole LH. Studies on radio-opaque polymeric biomaterials. Potential applications to endovascular prostheses. *Biomaterials* 1996; **18:** 1803–1812.
11 Benzina A, Kruft MAB, van der Veen FH *et al.* A versatile three-iodine building-block leading to radio-opaque polymeric biomaterials. *J Biomed Mater Res*, in press.
12 Kruft MAB, Koole LH. A convenient method to measure monomer reactivity ratios. Application to synthesis of polymeric biomaterials featuring intrinsic radio-opacity. *Macromolecules*, 1996; **29:** 5513–5519.
13 Horak D, Metalova M, Svec F *et al.* Hydrogels in endovascular embolization. III. Radio-opaque spherical particles, their preparation and properties. *Biomaterials* 1987; **8:** 142–145.
14 Hench LL, Wilson J. Surface-active biomaterials. *Science* 1984; **226:** 630–636.